

Experimental Evaluation of Out-of-Plane Strength of Masonry Walls Retrofitted with Oriented Strand Board

Ornella Iuorio^{a*}, Jamiu A. Dauda^a and Paulo B. Lourenço^b

^aSchool of Civil Engineering, University of Leeds, Woodhouse Lane, LS2 9JT, Leeds, United Kingdom

^b ISISE, Department of Civil Engineering, University of Minho, Azurém, P-4800-058 Guimarães, Portugal.

*Corresponding author: o.iuorio@leeds.ac.uk (O. Iuorio)

Email : cnjad@leeds.ac.uk (J.A Dauda), pbl@civil.uminho.pt (P.B Lourenço)

Highlight

- Unreinforced masonry (URM) walls are retrofitted using Oriented Strand Board (OSB).
- OSB type 3 improved the out-of-plane resistance and toughness of URM walls.
- The initial failure load is increased by 40% and 80% for 1 and 2-sided application.
- The deflection capacity of 2-sided is 50% more than that of 1-sided application.
- The estimated cost is 30% cheaper than fibre-based retrofit applications.

Abstract

Structural retrofitting is carried out as an economical alternative to demolishing and rebuilding existing masonry structures. Retrofitting is provided to offer structural upgrade and damage-control. This paper presents the application of oriented strand board type 3 (OSB/3) for retrofitting unreinforced masonry walls. Out-of-plane bending test in form of four-point loading was performed on six masonry walls. The test results show that OSB/3 can considerably increase the load and flexure capacity by (1.4 & 1.8), limiting-toughness by (1.6 & 2.4) and overall-toughness by (16 & 10) times compared to plain wall subjected to out-of-plane loading for (single & double-sided) application respectively.

Keywords

Unreinforced Masonry Wall

Retrofit

Oriented Strand Board

Out-of-Plane

Testing

Timber Panel

Load Capacity

Displacement

Toughness

1. Introduction

Masonry construction is a composite configuration of brick units and mortar bonded together. They can be classified as unreinforced, reinforced, confined, and prestressed depending on the engineering details involved in their construction. Among them, unreinforced masonry (URM) is certainly the most common typology adopted in historical constructions (1). URM construction contributes to a large proportion of the total building and infrastructure stock worldwide. Masonry construction has been largely adopted in many countries because of its low cost, ease of construction and building technology that uses recyclable resources, reduces waste, and creates a healthy environment, which are fundamental attributes of sustainable constructions (2). Despite these fascinating advantages of masonry constructions, most existing masonry structures were not designed in compliance to any code and their lack of proper structural detailing makes many of these heritage buildings vulnerable when subjected to even low-intensity out-of-plane loading (3). Therefore, structural retrofit is often necessary to allow URM buildings lasting to future generations. Structural retrofitting of URM structures is developed to increase structural capacity or to control structural damage of unreinforced masonry wall (4).

Generally, the structural failure mode of URM walls is classified as either in-plane or out-of-plane (5), (6) and (7). The in-plane failure mode is likely to be either bed joint sliding shear failure, diagonal tension (shear) failure, rocking or toe crushing (6). Meanwhile, the out-of-plane failure of URM walls is, usually, characterized by either one-way or two-way bending of the walls. The failure mechanism of masonry building can be local (mode I) or global (mode II) as shown in figure 1. These can result in a partial or total collapse of the wall (Fig. 2). Previous works (8), (9), (10) and (11) have demonstrated that URM walls are particularly susceptible to excessive out-of-plane loading. The major cause of out-of-plane failure of URM walls is their weaker resistance to out-of-plane loading. Although they have good resistance to gravity loads and compression (12), they are very weak in bending due to their limited ductility and lack of tensile resisting elements (9), (13) and (14). Out-of-plane failure of a structural URM wall is also caused by the lack of adequate building connections between the walls and floor diaphragms (15) and (16). Out-of-plane failure is the most devastating failure mode of URM walls and buildings (17) and (18). Hence, this research specifically aims to improve the out-of-plane capacity of URM walls.

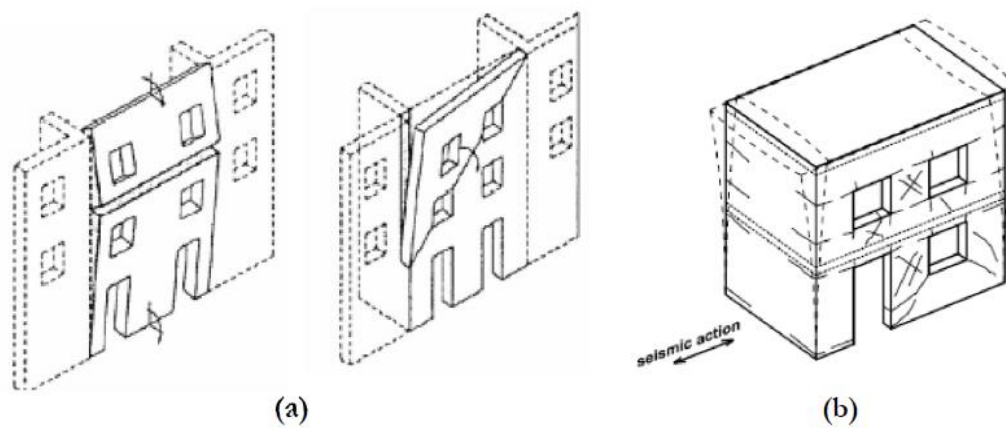


Figure 1. Failure mechanism modes; (a) Mode I: local (15), (b) Mode II: global (19)

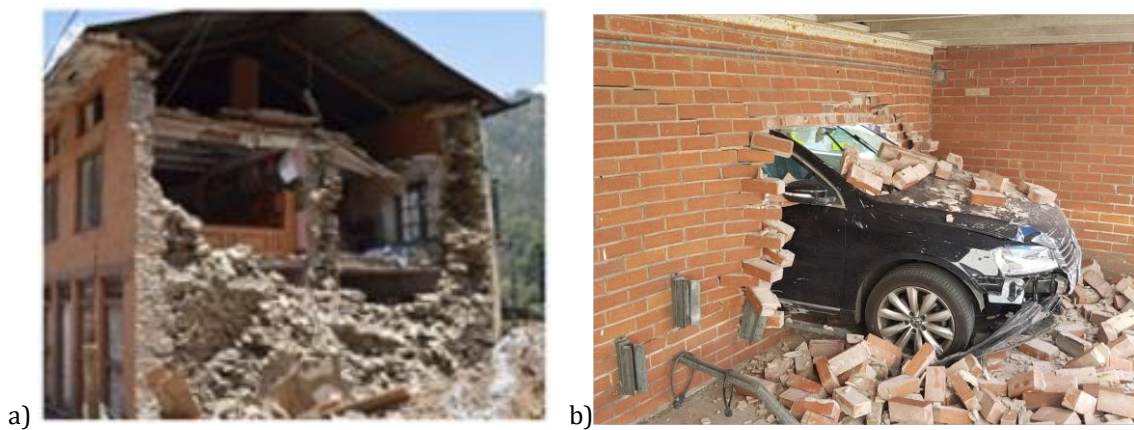


Figure 2. Examples of out-of-plane failure of URM due to (a) Excessive loading (20), (b) Car impact (21)

Over the years, several retrofit techniques have been developed to increase the load capacity of existing URM structures, meet the current load demand and prevent the aforementioned dangerous out-of-plane failure of URM walls. In the case of historical URM structures, retrofitting is aimed at making the building safer and less prone to major structural damage to preserve their culture and heritage significances (22). The existing retrofit techniques can be broadly divided into two categories: structural level and member level intervention. Structural level interventions often aim to tie structural and non-structural elements (e.g. non-load bearing partitions) together to allow the building developing a box-behaviour (23). Structural level interventions may include base isolation (24), energy dissipation devices such as dampers (25) and (26), floor/roof diaphragm action connectivity (23), reinforced concrete tie and masonry confinement (27) and masonry active tying branded as CAM arrangement in URM wall by Dolce, et al. (28).

Member level interventions aim to increase ductility and/or capacity of individual members such as floors and walls of existing URM buildings. The existing member level retrofit techniques are usually in the form of joint treatment (repointing and grout injection), surface treatment (coating and reinforced plaster), FRP wrapping (29), internal and external reinforcement (30) and other innovative techniques such as post-

tensioning (31), and *reticulatus* systems (32) and (33). The main benefit of member level retrofit in URM building is to bring the members to a condition that they will be sufficient for the intended structural service (34). Here, a new member level retrofit for URM walls, that adopt widely available wooden based panels, is addressed.

This present study proposes the application of timber panels to retrofit existing URM walls to improve their out-of-plane performance. Timber is one of the oldest structural materials used in many parts of the world. Timber is highly known for its relatively higher strength to weight ratio (35) compared to concrete and mortar coatings currently being used for retrofitting URM walls. It also has high shear strength across the grain, and good aesthetic compared to FRP wrapping and steels bracing system. Despite these obvious advantages of timber, the literature review shows that the potentials of timber have not been fully investigated in the structural retrofit of existing masonry buildings. Even though (11) and (36) have acknowledged the seismic performance of timber-framed structures during earthquakes, there is little evidence of using timber panel to retrofit existing unreinforced masonry building.

Timber-panels are currently being used for energy retrofit of existing buildings (37) and (38), but their capacity to also improve the structural strength of masonry walls has not been fully investigated. Very few experimental studies, (39) and (40) have exploited the strengthening of masonry walls using timber strong-backs while (41), (42) and (43) have analysed the application of timber panels as strengthening system for existing buildings against seismic force. The in-plane behaviour of URM retrofitted with Cross Laminated Timber (CLT) panel was studied, and the results showed that there is a considerable increase in the strength and ductility of the retrofitted wall. A 100% increase in ductility when the CLT panel is connected to URM walls with a specially developed steel connection at the top and bottom of the wall was observed (41). However, the application of CLT panels in existing masonry building can be challenging when considering the cost of CLT panels and the difficulty of applying them to any masonry building. Therefore, this study proposes the application of oriented strand board (OSB) type 3 panel to retrofit URM walls. OSB is regarded as a promising wood-based structural panel due to its superior strength, stiffness, workability, and competitive pricing (44).

This research investigated the performance of OSB type 3 panels connected to URM wall by threaded dry rod connections and injectable chemical adhesive anchor readily available in the European market. However, it is imperative to point out that the novelty in this proposed retrofit technique is different from the well-known timber-framed masonry (or half-timber) building (Fig. 3a). In timber-framed masonry building, the masonry wall is confined with the timber frame to enhance the stability and integrity of masonry walls for the in-plane and out-of-plane loads. Differently, the proposed technique considers securing timber panel behind the masonry wall (Fig 3b). In this study, 18mm thick OSB type 3 was connected to URM walls using $\varnothing 8\text{mm}/\text{L}50\text{mm}$ threaded anchor rods together with an option of plastic plug or injection mortar to investigate how the out-of-plane behaviour of the retrofitted URM wall changes under out-of-plane

loading. The study investigated only the out-of-plane performance of the proposed techniques because URM walls are more vulnerable when loaded in the out-of-plane direction and generate costly damages and losses of lives upon failure.

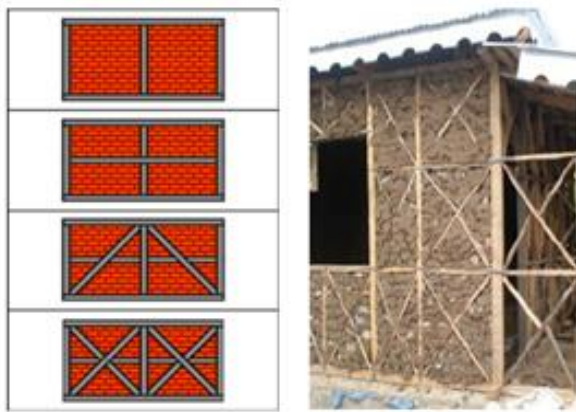


Figure 3a: Timber confinement of URM

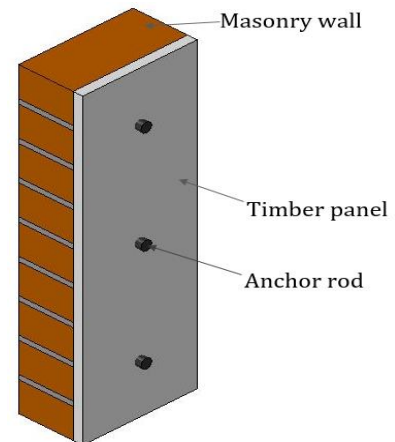


Figure 3b: Proposed timber panel retrofit

This paper presents experimental works on large-scale (1115 x 1115 x 215mm) masonry walls. Considering the good results obtained by earlier studies, (45) and (46) on the investigation of timber-masonry composite retrofit for small-scale single leaf URM prisms, this paper investigates the applicability to large-scale walls. This study presents the quasi-static out-of-plane loading test on plain masonry wall specimens, single-sided retrofitted masonry walls and double-sided retrofitted masonry walls. The load and displacement capacities, flexural strength and toughness were evaluated in both plain and retrofitted specimens, and the results were analysed and discussed. The experimental works involved subjecting both plain and timber retrofitted URM walls to out-of-plane loading using quasi-static (monotonic) loading scheme. The reasons for selecting the quasi-static loading scheme is that the test will be able to replicate the behaviour of URM wall when subjected to monotonic or cyclic loading through a hydraulic actuator, which is similar to what is expected from the effect induced by wind, explosion or earthquake. Quasi-static loading has been widely accepted and implemented in previous studies in the absence of shaking table facilities (9), (47) and (48). Meanwhile, this study is not exclusively applicable to earthquakes but to generate knowledge and understanding of whether timber panels can improve the capacity of URM walls against excessive out-of-plane loading from multiple actions.

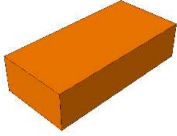
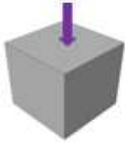
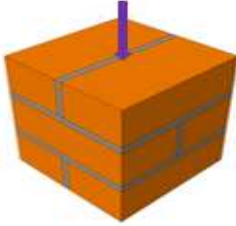
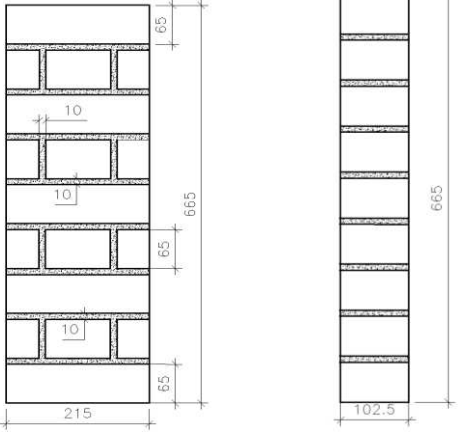
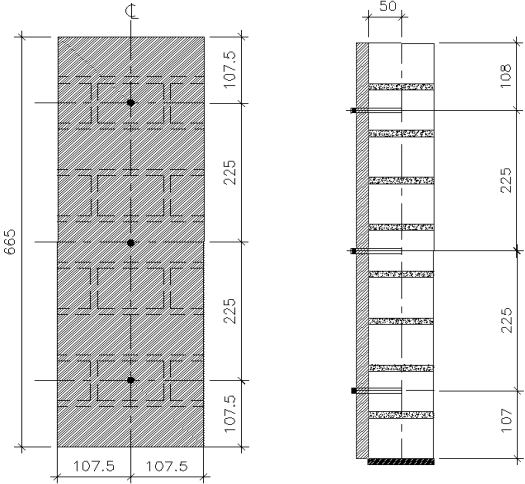
The paper is articulated in four different sections. After this introduction (section 1), the experimental tests set up and instrumentation to assess the efficiency of the retrofit technique is presented in section 2. Section 3 presents the analysis and discussion of the test results. Conclusion and future research development are given in section 4.

2. Methodology

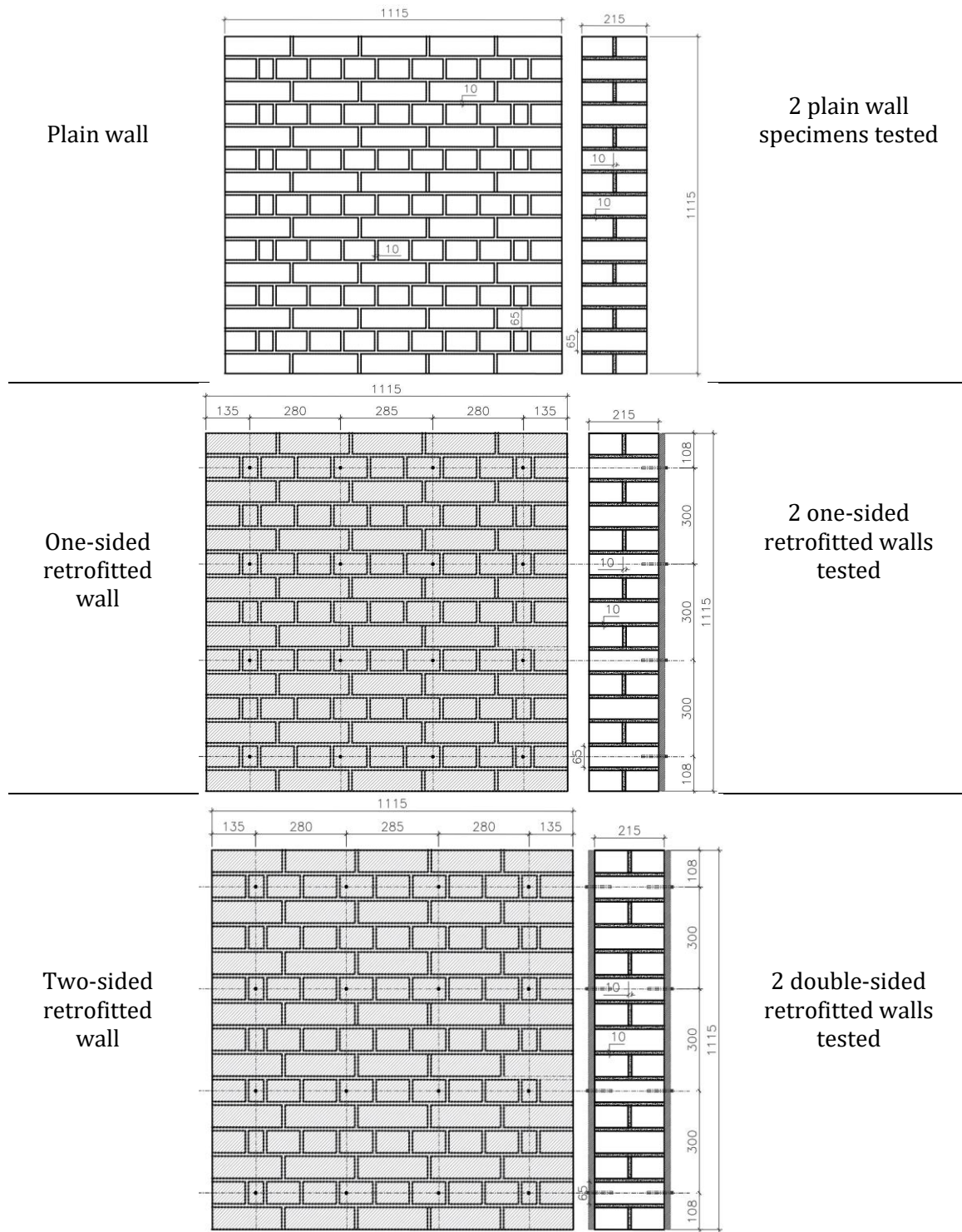
The integrated approach adopted in this study has been articulated in table 1 into three key stages: (I) experimental characterisation of masonry components (45) and (49); (II)

out-of-plane flexural bond strength tests on 665 x 215 x 102.5mm masonry prisms (46); and (III) out-of-plane testing of 1115 x 1115 x 215mm masonry walls (50).

Table 1. Full experimental matrix

Stage I: Material Characterisation		
Brick Unit		Brick units tested for dry density, water absorption, compressive strength, modulus of elasticity and Poisson's ratio
Mortar		Fresh mortar tested for consistency: dropping ball and flow table test. Harden mortar cube tested for compressive strength
Masonry Cube		Masonry cubic specimens tested for compressive strength
Stage II: Small-Scale Test (Flexural bond strength of masonry prism, MP)		
Plain MP		3 plain MP specimens to be tested
Retrofitted MPOSB		<p>3 MP specimens retrofitted with C1: adhesive anchor</p> <hr/> <p>3 MP specimens retrofitted with C2: mechanical connection</p>

Stage III: Large-Scale Test (Flexural strength of masonry wall)



The full description of the second phase which precedes the study presented in this paper can be found in (46). The second phase showed that the application of OSB panel at the back of masonry prisms greatly influenced its out-of-plane behaviour. In plain masonry prisms (MP), the collapse was sudden with the evolution of crack opening in a single mortar bed joint within the inner bearing of the specimen. The failure (cracking) of the

MP specimen occurred abruptly between the interface of the mortar joint and brick unit. While, in the retrofitted specimen (MPOSB), the OSB panel improved the flexural response of the specimens such that the failure was much more ductile. Indeed, the retrofitted MP is able to offer flexural strength to resist out-of-plane load almost 7.5times greater than plain MP in case of adhesive anchor (C1) and 5.0times greater when a mechanical connection (C2) was used. Adhesive anchors performed thus much better for the envisaged application. Consequently, the out-of-plane displacement showed in retrofitted MPOSB is almost 2.0times greater than that of plain MP. This is because there is limited tensile strength in plain MP and the failure (collapse) is sudden. But the addition of OSB panel offered additional tensile strength and ductility in retrofitted specimens, and thus they were able to displace gradually before the timber failed. The performance of the proposed retrofit technique recorded in small scale testing might have been amplified due to the fragility of the plain specimen, which is not a true representative of the real working condition of URM walls. As such, a large-scale experimental campaign on 1115 x 1115 x 215mm single leaf, double wythe solid URM walls carried out in stage 3 to study the proposed technique in detail.

This paper presents and discusses the phase 3 of the experimental testing. Several previous experimental works (7) (9), (17), (41), (47), (48), (51), (52), (53), (54), (55), (56) and (57) have assessed the out-of-plane performance of URM walls. Their review and study have been instrumental in defining the geometry, URM walls boundary conditions, loading and general testing procedure for the testing of the retrofit technique proposed. The reviewed experimental works excluding that of (55) have been carried out on wall panels without returning walls at the corners. Although (55) geometric configuration is ideal for reproducing the in-situ condition of a portion of a typical load-bearing wall including corners, evidences from the previous works have shown that test on panels without corners is a good indication in assessing the out-of-plane capacity of URM walls. Hence, the walls tested in this study were without returning walls. The general boundary conditions assumed in the reviewed testing works were restraints at the top and bottom of the wall, which allowed the vertical strips of the wall panel to deflect in the out-of-plane direction. Since this study aimed to propose a retrofit technique that will improve the performance of URM walls against out-of-plane failure, it is thus imperative to assess the out-of-plane performance of plain and retrofitted URM wall to evaluate the improvement due to the application of the proposed retrofit technique. To do this, test setup which is similar to that of (7) and (52) which is according to ASTM procedures (58) and (59) was adopted in this research.

2.1 Test Specimens Constituents

The test specimens were constructed using engineering class B solid fired clay bricks with UK standard size 215 x 102.5 x 65mm and Type N (general purpose) mortar mix with a ratio of 1:1:6 (Type II Cement: aerial lime: sand) in volume. For the retrofitted samples, 18mm thick OSB type 3 and 8mm diameter adhesive anchors (made with a threaded dry rod with injectable chemical adhesive) were used. The OSB is manufactured from strands

of wood, which are bonded together with a synthetic resin (60). The OSB panel was securely connected behind the masonry wall using an adhesive anchor connection, which is a combination of styrene-free vinylester-hybrid injection mortar and A4 anchor rod. A4, or 316, is the marine grade of ISO 3506 stainless steel. The styrene-free vinylester-hybrid mortar is a high-performance injection mortar, which is approved for fixings in both perforated and solid brick. The adhesive anchor connection has been identified as the best-performed connection from the connection type studied in the small-scale test campaign described by (46). The criteria for selecting the connection type are guided by the requirements of European Technical Approval (61), which ensure that the selected anchorages are fit for use in solid masonry subjected to either static or quasi-static loading which was tested in this study. The strength of both the masonry unit and mortar were considered in the selection of the anchor diameter. The spacing of the anchors is provided to meet the minimum allowable spacing and edge clearance as specified in the ETAG 029 (61). The general materials properties as determined by (49) are reported in table 2.

Table 2. Properties of used materials

Properties	Masonry Unit	Mortar	OSB	Anchor
Mass density (γ) kg/mm ³	2.20e-6	2.17e-6	0.65e-6	7.85e-6
Young modulus (E) N/mm ²	32470	19850	3500	210000
Poisson ratio (μ)	0.26	0.20	0.24	0.30
Compressive strength (f_c) N/mm ²	87.9	7.1	6.6	-
Tensile strength (f_t) N/mm ²	5.93	0.32	0.92	-

2.2 Test Specimens Construction Details

Six single leaf, double wythes URM wall specimens measuring 1115 x 1115 x 215mm (length x height x width) were constructed. The selected geometry of the walls is such that each of the two wythes of the walls has 15 courses with each course having 5 units of brick bonded together by 10mm thick mortar joint. The walls were built in English bond consisting of alternate rows of headers and stretchers, which is the oldest form of brick bond popular in the UK since the late 17th century (62). The bonding pattern is such that the joints between the stretchers are centred on the headers in the course above as can be seen from the plan sketches of first and second courses of the bonding pattern in figure 4a and the image in figure 4b.

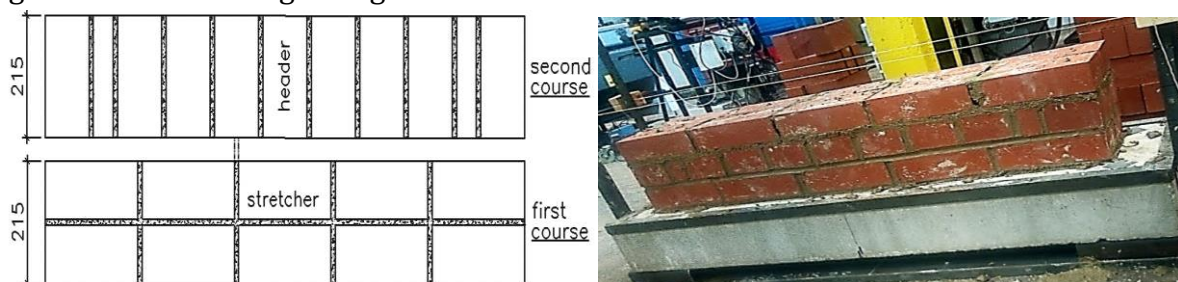


Figure 4. Wall specimen bonding pattern (a) plan drawing, (b) image during construction

For the retrofitted wall specimens, brick units were pre-drilled in specific locations and bonded to have a connection layout as shown in figure 5. The connection layout ensured that the spacing of the connections has 50mm as minimum edge clearance and 250mm as the minimum spacing between two connections. All wall specimens were constructed on 1315 x 150 x 350mm (length x height x width) reinforced concrete (RC) footing with 1mm thick polymer (nylon) placed on top of the RC footing to prevent the bottom of the wall from bonding to the RC and to avoid toe crushing failure during testing. The wall specimens (Fig. 6) were constructed and tested in place to avoid causing disturbance to the specimens when moving to the test rig. All walls were cured by wrapping them with a polythene sheet for 14 days and then cured for further 14 days in the open air in the laboratory. For the retrofitted masonry wall, the OSB timber panel was fixed to the masonry walls after 21 days to allow for curing of the injection mortar in the connection point.

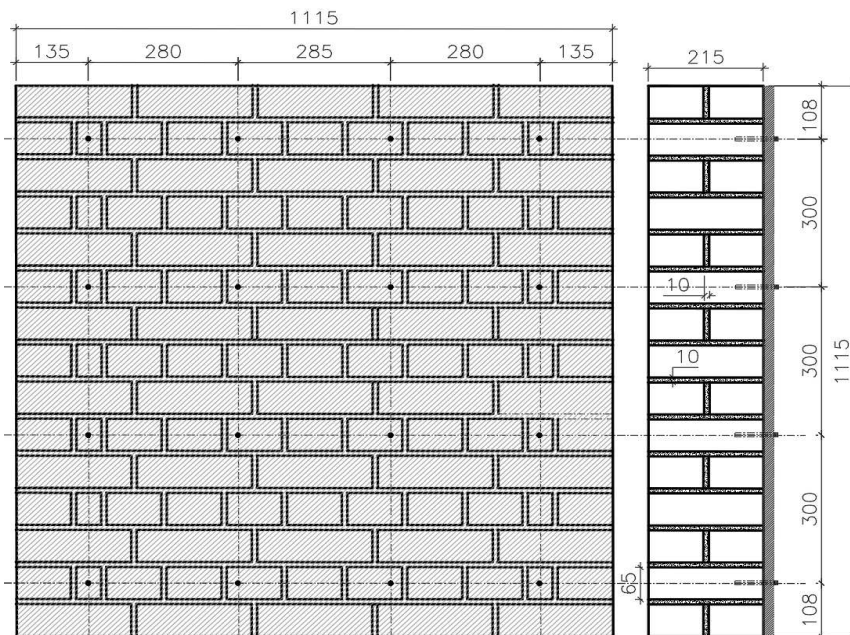


Figure 5. Typical connection layout for retrofitted wall specimens (all dimensions in mm)



Plain wall



1-sided retrofitted wall



2-sided retrofitted wall

Figure 6. Masonry wall specimens (as-built)

2.3 Test Program

Out-of-plane load control tests have been performed on six masonry wall specimens, as indicated in table 3. Two walls identified as PW1115-1 & 2 were tested as plain specimens. For the retrofitted specimens, two samples were tested as single-sided retrofitted samples (1SRW1115-1 & 2) while the last two samples were tested as double-sided retrofitted (2SRW1115-1 & 2). The test program has ensured that loading has been applied on wall retrofitted with OSB panel on only tension face (1SRW) and both tension and compression faces (2SRW) of the masonry wall. This is because one possible application of the proposed technique is to use the OSB panel on the internal surface of exterior URM walls so that the external appearance of the building is preserved. The other retrofit configuration is the application of the OSB panel also on the outer surface of exterior URM walls with the combination of plaster, brick-polymer based imitating finishing or clay tiles. The configuration with the OSB on both sides holds walls when heritage values are less stringent, and the solution is feasible.

Table 3. Test program for out-of-plane wall tests

Specimen designation	Description
PW1115-1 PW1115-2	Plain masonry wall specimen to serve as baseline line for evaluating the retrofit performance
1SRW1115-1 1SRW1115-2	Masonry wall retrofitted on one side using the OSB panel and adhesive anchor
2SRW1115-1 2SRW1115-2	Masonry wall retrofitted on both sides using the OSB panel and adhesive anchor

PW stands for Plain Wall
1SRW stands for 1 Side Retrofitted Wall
2SRW stands for 2 Sides Retrofitted Wall

2.4 Test Setup and Procedures

The general test setup (Fig. 7 & 8) was designed to replicate a four-point loading test arrangement, which is suitable for assessing the flexural behaviour of masonry wall as described in (58). Each wall specimen was tested by applying an out-of-plane load in the middle section of the wall to induce a constant flexural bending moment in the central area of the wall. The load was applied to each tested specimen using a hydraulic ram and was distributed through a steel spreader arrangement in the central area of the wall (Fig. 8b). The spreader arrangement spanned between the fourth courses from the top and bottom of the wall specimen. All specimens were tested with simply supported boundary condition and a (slight) vertical pre-compression load on top of the walls.

The simply supported boundary condition of the specimen was achieved by supporting the back of the wall across the middle of the top and bottom course with backing steel frames. The backing frames were connected to an existing stanchion as a reaction frame at the top and bottom of the wall (Fig. 8c). A 25mm diameter roller was placed between the back face of the wall and the supporting steel plate on the reaction frames to provide

for smooth distribution of load action across the length of the wall and avoid point contact. On the front side of the specimen, two metal plates (50 x 5mm thick) were fixed at 1/4th and 3/4th of the height of the specimen each to provide a contact for the roller on the steel load spreader arrangement.

All the test arrangements were carried out while the specimen constructed on the RC footing still rested on the four 60mm square pipes placed at each corner of the RC footing. These square pipes identified with square shape at the bottom of the footing in figure 7 ensured that the wall was stable during preparation. This also allowed the placement of 50mm diameter roller under the specimen before the start of the load application. Once the setup was completed, the 50mm diameter roller was slid under the specimen, and the four 60mm square pipes were removed. This allowed the wall specimen to rest on the 50mm diameter cylindrical roller (Fig 8d), with the axis of the roller parallel to the specimen's face to allow it to freely rotate around its base while deflecting out-of-plane and preventing any restrained end condition.

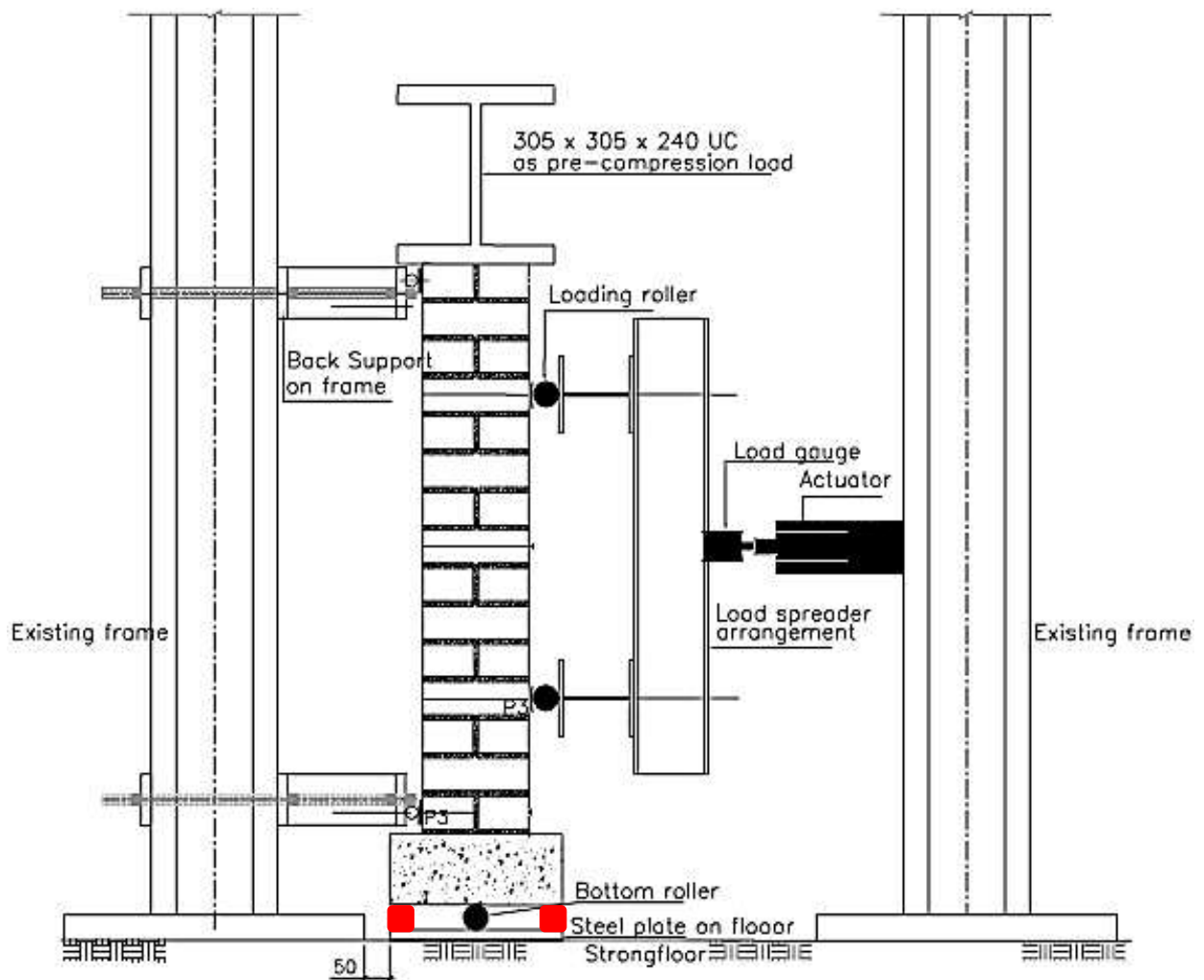


Figure 7. Out-of-plane testing arrangement (drawing scheme)



a) Side view showing the general test arrangement



b) Front view showing loading area



c) Back view showing upper and lower support



d) Roller under wall specimen

Figure 8. Out-of-plane testing arrangement (as-built)

2.4.1 Loading Procedures

The direction of the load application was perpendicular to the wall specimen surface. The test was load controlled, and the loading scheme was such that an initial load was applied continuously at a rate of 1kN/min for up to 5kN and then maintained the load for 5mins period. The purpose of maintaining the applied load was to allow the wall assembly to come to substantial rest before taking the next set of reading as recommended in (58). Also, this helped to observe any time-dependent deformation and load redistribution. The load steps were repeated continuously for 10kN, 15kN, 20kN, 25kN, and 30kN load and maintained for 5mins period at each load step (Fig. 9). After that, the load was increased continuously to the failure of the test specimen. To obtain the maximum capacity of the retrofitted walls, the applied load was increased continually after the first crack until additional cracks were formed in the retrofitted specimens and ultimately the timber at the back of the masonry walls was broken. For the constant pre-compression load, a 305 x 305 x 240 UC section amounting to 3kN load was placed on top of the wall (i.e the self-weight of the steel beam). The pre-compression load applied simulated a vertical load on the wall, e.g. due to a light roof, and was adopted for increasing the stability of the testing.

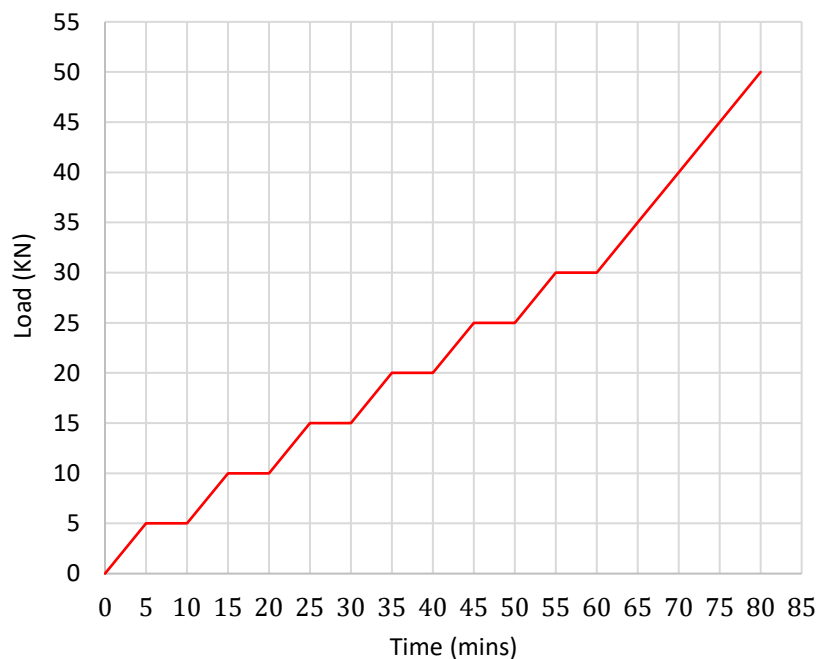


Figure 9. Applied out-of-plane load history.

2.4.2 Instrumentation

The values of the applied load on the wall were monitored using a 200kN capacity ring load cell. Simultaneously, 8 linear variable displacement transducers (LVDTs) were used to record the deflections of the test specimen along the wall centre (LVDT1, 2, 3 and 4), top (LVDT 5 and LVDT7) and bottom (LVDT 6 and 8). The locations of these gauges were as shown in figure 10. All the eight LVDTs used during the test were fixed on an independent steel tripod stand, which was not connected to the test rig. For the plain walls and one-sided retrofitted wall, the LVDTs were applied directly on the face of the

brick unit at the respective location identified in figure 10. While in the double-sided application, the LVDTs were applied to the timber panels at the same location identified in figure 10. The force and the displacements were real-time monitored by connecting the measuring equipment (load cell and LVDTs) to an electronic acquisition unit interfaced with a computer.

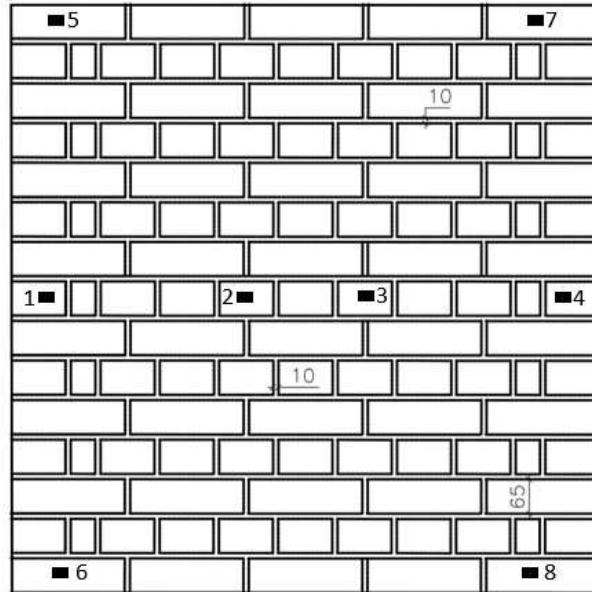


Figure 10. Position of LVDTs on wall specimen

3. Results Analysis and Discussion

The experimental results were expressed in terms of load vs displacement curve representing the total applied out-of-plane load against the net out-of-plane displacement for both plain and retrofitted specimens. The performance of the plain specimens was analysed as the baseline for estimating the effectiveness of the proposed retrofit technique.

The net out of plane displacement in the mid-height of the wall was estimated by deducting the mean displacement recorded at the top and bottom of the specimens from the average mid-height displacement. This deduction accounted for any small displacement at the top and bottom of the wall.

Here, the wall was considered as a single part with three regions as the top, mid and bottom. In order to estimate the net displacement in the specimen mid-height, the average value of horizontal displacement at the top and bottom of the specimen was removed from the mean value of the displacement measured at the specimen mid-height using equations 4 to 7.

$$d_{net/top} = \left(\frac{d_5 + d_7}{2} \right) \quad (4)$$

$$d_{net/bottom} = \left(\frac{d_6 + d_8}{2} \right) \quad (5)$$

$$d_{net/mid} = \left(\frac{d_1 + d_2 + d_3 + d_4}{4} \right) \quad (6)$$

$$d_{net} = d_{net/mid} - \left(\frac{d_{net/top} + d_{net/bottom}}{2} \right) \quad (7)$$

Where d refers to displacement at a particular position of LVDT as shown in figure 10.

3.1 Plain Masonry Walls

Throughout the loading steps, out-of-plane loads and the corresponding net out-of-plane displacements were obtained and presented in the form of the load-displacement curve (Fig. 11). The observed failure pattern (Fig. 12) in the plain walls is characterised by the sudden formation and rapid opening of the crack in the unit/mortar joint interface throughout the thickness of the walls. The failure of the plain masonry wall is quasi-brittle and started with the formation of a crack opening in one bed joint at the tensile face of the walls (i.e. the side opposing the loading face). Subsequently, this crack was propagated through the perpendicular joint to the next bed joint (Fig 12b). The crack occurred throughout the whole thickness of the wall and led to the complete separation of the unit-mortar interface at the failure load (maximum load the wall can resist). In the case of PW1115-1, the pre-compression load applied varied according to the applied out of plane loading during testing because an hydraulic jack was used to imposed additional 7KN load to the 3KN (i.e. the self-weight of 305 x 305 x 240 UC) on top of the wall. However, the hydraulic jack used to simulate the pre-compression load was unstable. Thus, PW1115-1 experienced an increasing axial compressive stress after the first crack. This loading effect makes PW1115-1 fail in multiple bed joints as highlighted in figure 12a (image taken at the end of the test when the out-of-plane load has been released and the wall returned to its original position with the cracks closed up). In PW1115-2, the self-weight of the steel beam on the top of the wall is the only additional compressive load on the wall, which is the configuration adopted in all other tests. Therefore, the result of PW1115-1 is only valid until the first crack occurs.

The analysis of the load-displacement curve (Fig. 11) shows that the two plain specimens have a quasi-linear behaviour up to about 15000N load, which corresponds to the onset of crack formation in PW1115-2. After that, the load continuously increased with a little increase in the out-of-plane displacement before the specimen failed. At the failure point, the displacement suddenly increased. This increment is due to the brittle nature of the failure pattern. The maximum load attained by PW1115-2 is 38330N and the corresponding net out-of-plane displacement at this point is 5.25mm. Meanwhile, PW1115-1 appeared very stiff after first crack (Fig. 12a) with increased bending capacity because the axial load keeps increasing as the horizontal load increases, preventing significant out of plane displacements. At about 25000N load capacity, there is an onset of crack 1 in the specimen, which later failed at maximum load of 39720N with a corresponding net out-of-plane displacement of 3.4mm. Then, because of the increasing pre-compression load, there is a redistribution of the stresses in the wall, which then allowed PW1115-1 to carry more out-of-plane load until crack 2 formed at 65000N applied out-of-plane load.

Clearly, the applied load on PW1115-1 has passed the normal load capacity of the wall, which is 38330N for PW1115-2. So, the loading was stopped after the failure of crack 2.

This was to avoid the total collapse of the wall and damage of the instruments. It was evident that the higher axial load increased the out-of-plane capacity of the wall. However, the increasing axial load as the out-of-plane load increases is less realistic. Therefore, the load at the first crack of PW1115-1 (39720N) and the maximum load of PW1115-2 (38330N) are considered as the maximum load capacity of the plain specimen. The average of these two values (39025N) was chosen as a baseline to evaluate the effectiveness of the proposed timber-retrofit technique for both single-sided and double-sided retrofitted walls.

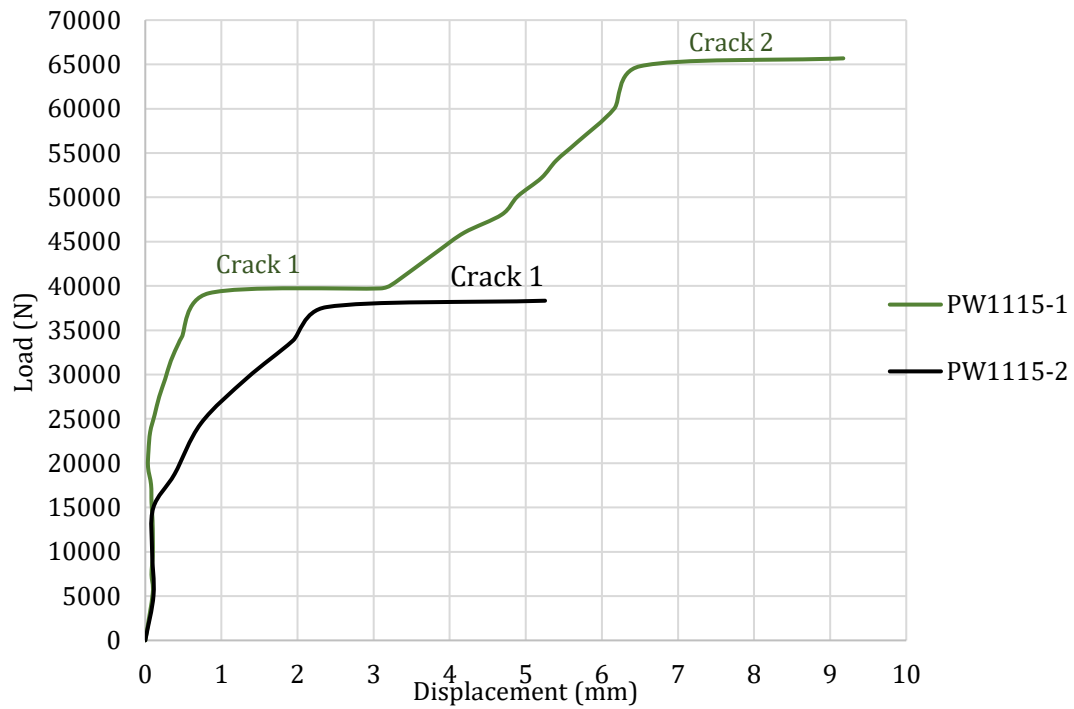
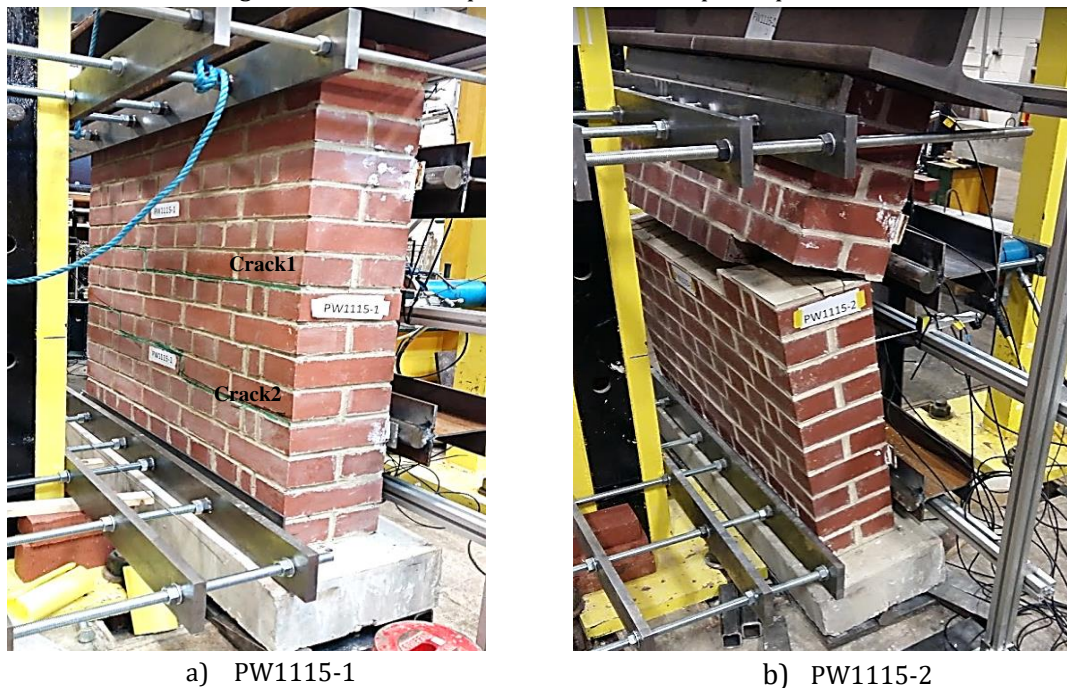


Figure 11. Load vs Displacement curve for plain specimens



a) PW1115-1

b) PW1115-2

Figure 12. Failure patterns of PW1115-1 & 2

3.2 Retrofitted Masonry Walls

Walls 1SRW1115-1 & 2 were retrofitted by the application of an OSB panel with adhesive anchors on the tension face of the wall (back). The behaviour of the single-sided application (1SRW) indicates that damage was delayed with important displacement at the occurrence of the first visible crack. The failure began from the tensile face with the first crack occurred in the unit-mortar interface at 54600N and 50900N with a corresponding out-of-plane displacement of 7.0mm and 6.2mm for 1SRW1115-1 and 1SRW1115-2, respectively. The average load and displacement equal to 52750N and 6.6mm, respectively

Meanwhile, walls 2SRW1115-1 & 2 had the application of OSB panels on both sides of the wall. The double-sided retrofitted wall (2SRW) shows minor displacement (0.25mm) before the first visible crack occurred in the masonry part at 70200N and 67200N for 2SRW1115-1 and 2SRW1115-2, respectively. This implies that the addition of the timber panel on the compression face (i.e. the face where the load was applied) improved the lateral resistance of the specimens. So, double-sided application means that the specimen remained almost undeflected and undamaged before the first crack occurred at an average load and displacement equal to 68700N and 4.2mm, respectively.

For the sake of comparison, the load-displacement curve of plain walls is included in figure 13, with PW1115-1 shown up to crack 1 formation only. This is because the additional strength gained by PW1115-1, which led to the formation of crack -2 was due to the increased axial load, which is not available on the retrofitted samples. An inference from figure 13 reveals that the proposed retrofit technique has substantially increased the out-of-plane load capacity of retrofitted walls. Specifically, 1SRW and 2SRW attained an average of 114600N and 120600N maximum load. Remarkably, the load capacity of the retrofitted walls before the first crack occurred is much higher than the maximum load capacity of the plain wall as discussed in detail below. On the load-displacement curve, the points at which the cracks occurred in the walls were indicated with numbers. This numbering corresponds to the numbers marked on the images from the test (Fig 14). For instance, a second crack at 81765N load and a third final crack at 116400N for 1SRW1115-1.

Evidently, the proposed timber retrofit technique has improved the brittle behaviour of the plain masonry wall. Unlike the plain masonry walls, the retrofitted masonry walls remained unseparated after the first crack. This is because the application of the OSB timber to retrofit the walls has improved the out-of-plane behaviour and integrity of the retrofitted walls. The retrofitted specimens displaced more in the out-of-plane direction, avoiding the sudden collapse of the walls. Figure 13 clearly showed that the proposed retrofit solution has increased the out-of-plane strength and displacement capacities of URM walls. It is worth to notice that observations about the post-peak behaviour cannot be made since the tests are load controlled and the loading was stopped after the failure

of OSB timber applied on the retrofitted walls. This procedure was adopted to avoid the total collapse of the walls and damage of the instruments.

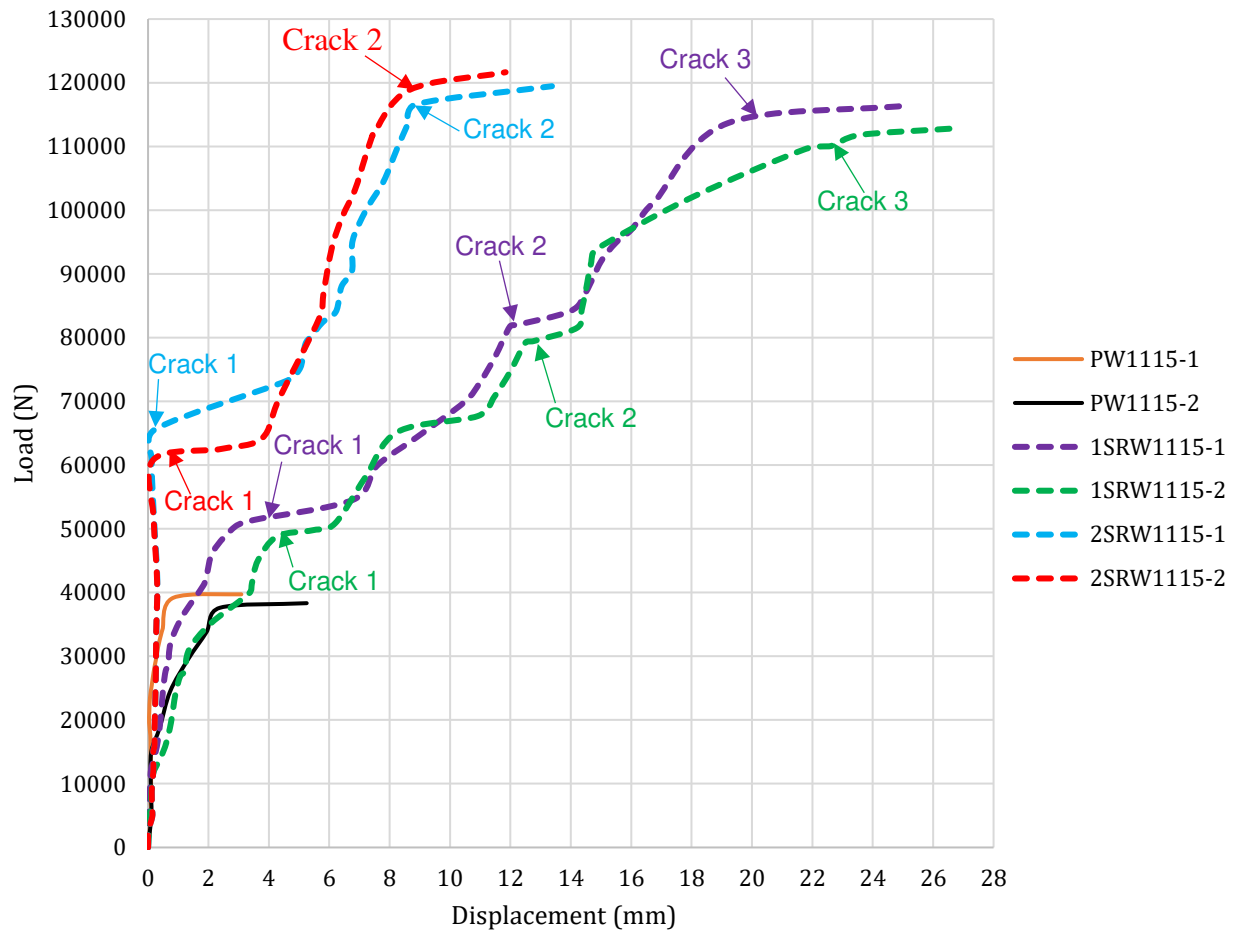
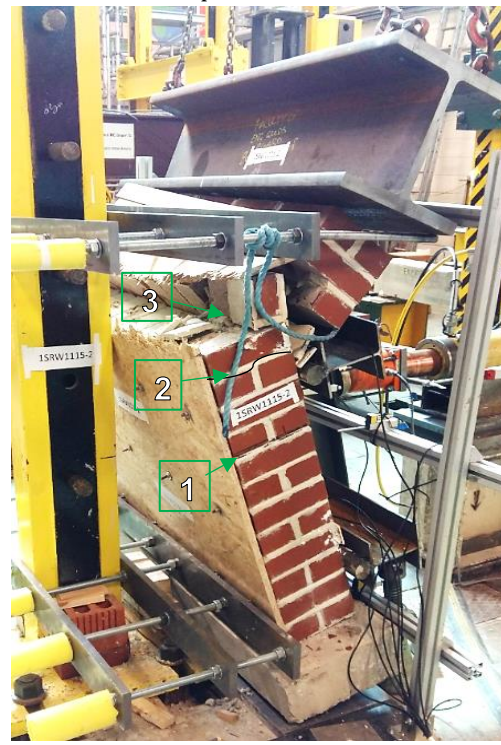


Figure 13. Load vs Displacement curve for specimens



1SRW1115-1



1SRW1115-2

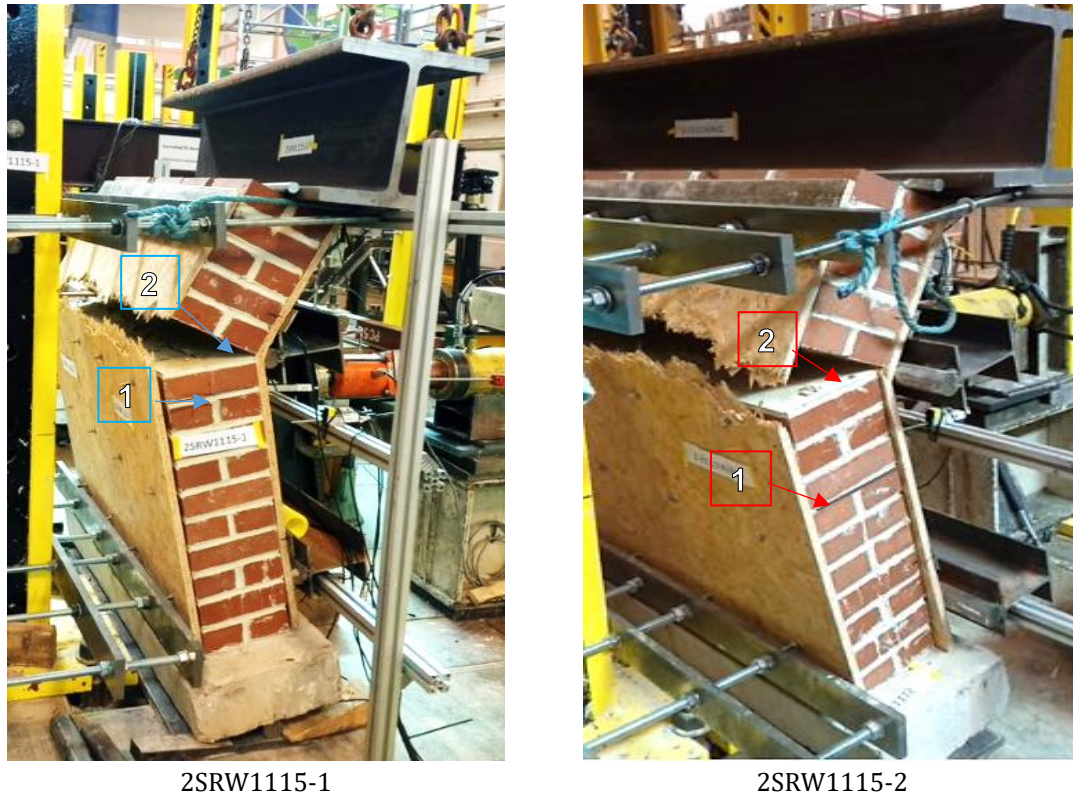


Figure 14. Failure pattern of retrofitted masonry wall

3.3 Performance of the Proposed Timber Retrofit Technique

The main results of the out-of-plane bending test in term of the first/initial visible cracking, failure load, their corresponding displacement, and toughness of the tested specimens are presented in table 3. The toughness (i.e. energy absorbed) of the specimens is estimated from the load-displacement curve in figure 13 using the method based on ASTM 1609 (63). The toughness is calculated in two stages, which are overall and limiting toughness. The overall toughness is estimated as the total area under the load-displacement curve while the limiting toughness is the area under the curve up to a limited displacement of the clear height of the wall divided by 250 (64). The purpose of estimating limiting toughness is to understand the toughness gained by the specimens when undergoing an acceptable displacement without adverse effect. The excessive displacement observed for the masonry walls tested before getting to the failure of OSB, and associated with the evaluated overall toughness, is not acceptable in any real situation, since it would lead to damage of building parts. Thus, the limiting toughness estimates the actual improvement due to the retrofit application in the acceptable range.

Thereafter, comparison charts at the occurrence of first crack (Fig. 15) and failure (Fig. 16) were developed for the performance evaluation of the proposed retrofit technique. The average load and displacement for each group of specimens (i.e. PW, 1SRW and 2SRW) were used to develop the charts. The comparison in term of capacity at the first crack (Fig. 15) shows that the load that caused the first crack in 1SRW is 1.4times the

maximum load at the failure of PW. Also, the first crack on the 2SRW specimen occurred at a load that is 1.8times the failure load of PW. This shows that the 2SRW resist more load before the first crack, about 1.4times that of 1SRW. At the failure point, the maximum load capacity of masonry wall retrofitted with OSB panel is 2.9times and 3.1times that of PW for 1SRW and 2SRW respectively (Fig 16). Unlike the load at the first crack, the load capacity of 2SRW is only 1.04 times that of 1SRW.

Also, the analysis of the test results shows a significant increase in the out-of-plane displacement of retrofitted walls. This is due to the application of the OSB timber panel that has offered the masonry wall a significant lateral resistance once the masonry joint interface cracked. As such, the retrofitted specimens were able to take more loads and absorbed more energy by displacing more without sudden failure. The increment in the out-of-plane displacement of the retrofitted walls is 6 times and 3.1 times that of PW for 1SRW and 2SRW, respectively.

The overall toughness gained due to the retrofit application when taken up to the failure of the OSB is enormous. An improvement of 16 times and 10 times that of the plain wall is estimated for application on single and both sides, respectively (Fig. 17a). However, the performance of the technique at the limiting displacement (Fig 17b) is otherwise with the double-sided showing more toughness gained than one-sided application (2.4xPW and 1.6xPW for double and single-sided application respectively). The analysis shows that the double-sided application offers the largest improvement in terms of toughness at the limiting displacement. Thus, the double-sided is the best option when higher energy absorption is required in a real situation.

Table 3: Performance of the proposed retrofit techniques

Specimen Label	First crack		Failure		Toughness (Nmm)	
	Load (N)	Disp. (mm)	Load (N)	Disp. (mm)	Limiting	Overall
PW1115-1			39700	3.40	112000	115000
PW1115-2	The first crack is the failure point		38300	5.25	118000	122500
Average			39000	4.33	115000	118800
1SRW1115-1	54600	7.00	116400	25.20	186000	1920000
1SRW1115-2	50900	6.20	112800	26.55	178000	1965000
Average	52750	6.60	114600	25.88	182000	1942500
2SRW1115-1	70200	4.58	119500	13.38	260000	1205000
2SRW1115-2	67228	3.78	121700	11.84	280000	1190000
Average	68714	4.18	120600	12.61	270000	1197500

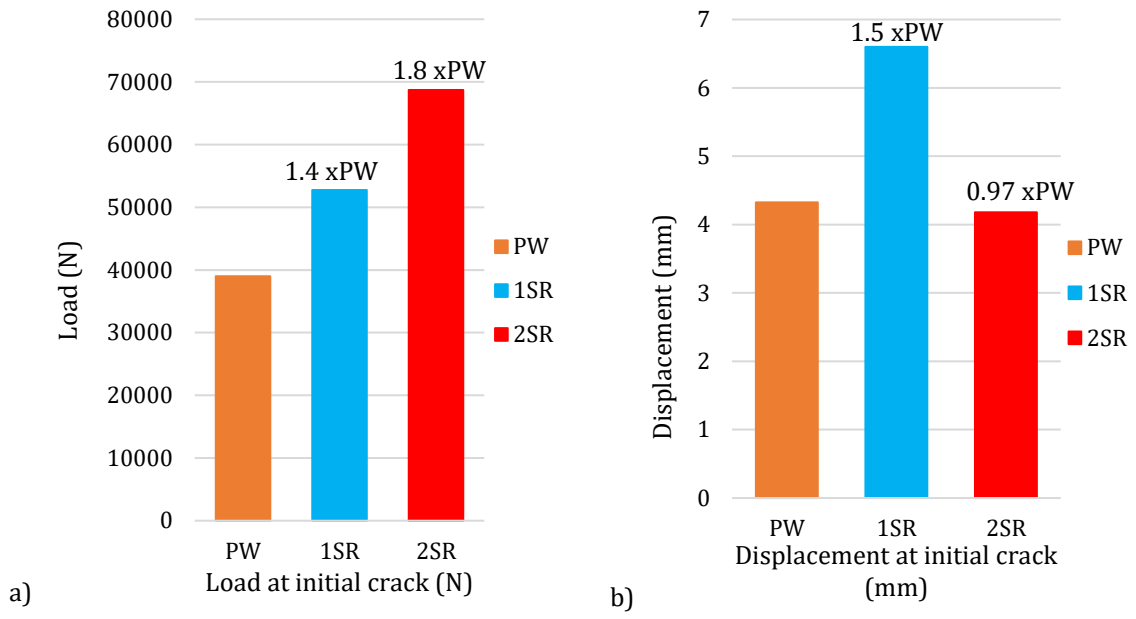


Figure 15. Performance at the occurrence of the first crack; (a) Load capacity (b) Displacement

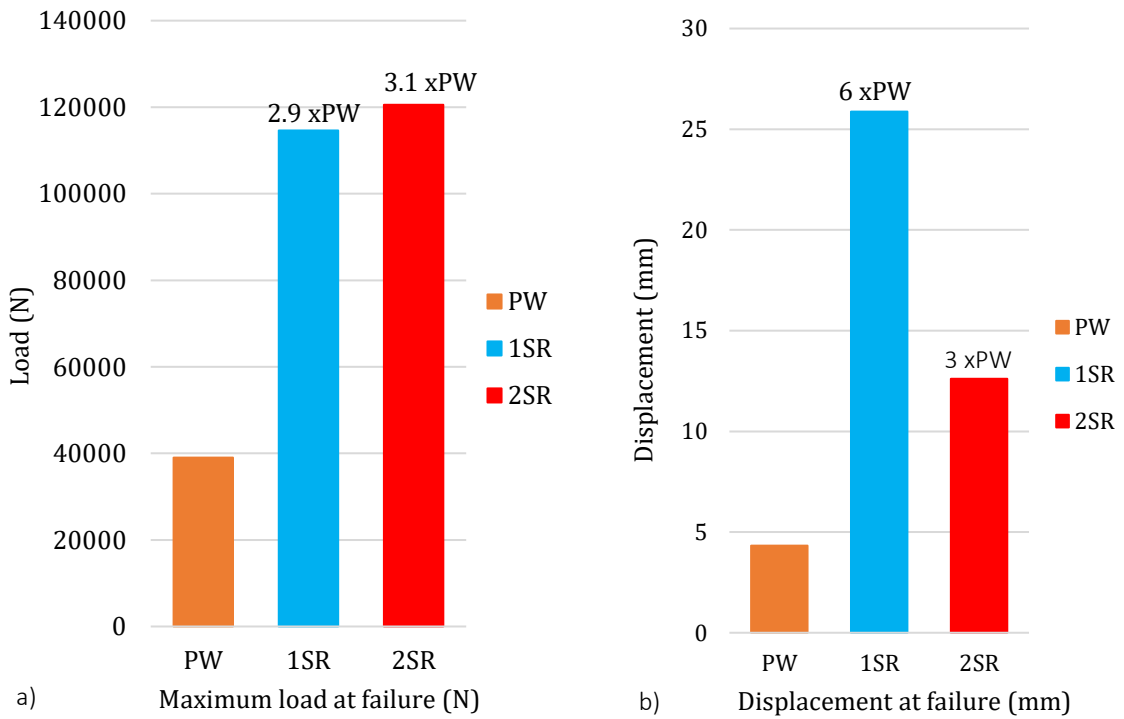


Figure 16. Performance at the failure; (a) Load capacity (b) Displacement

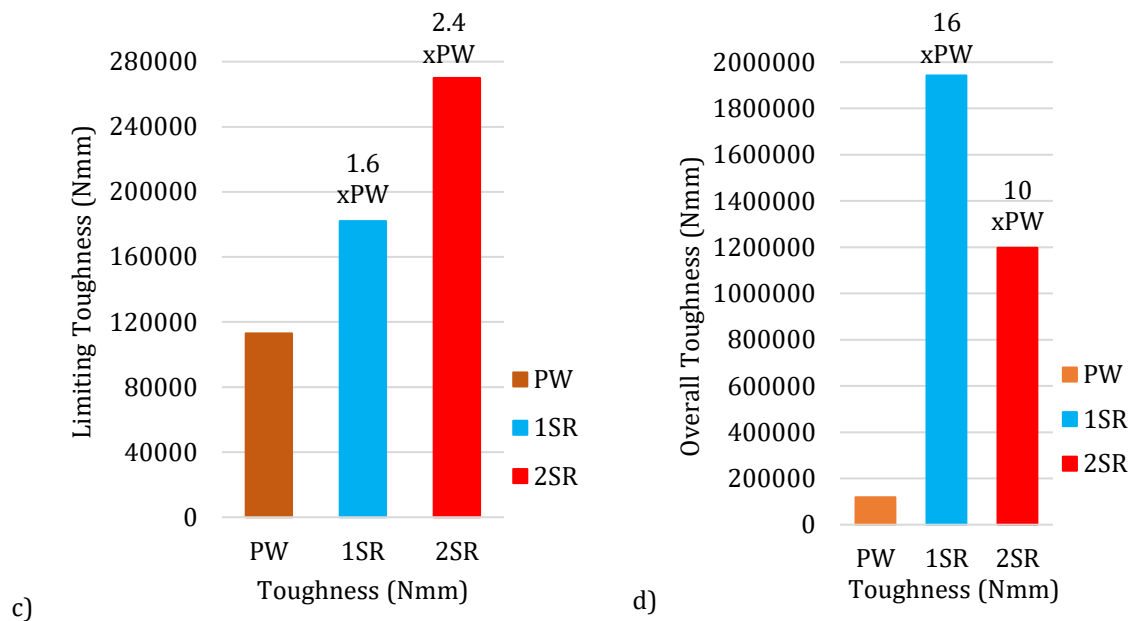


Figure 17. Performance at the failure; (c) Limiting Toughness (d) Overall Toughness

3.4 Comparison with Alternative Retrofit Techniques

Table 4 provides a comparison of the proposed techniques with few selected retrofit techniques found in literature (65), (66), (67)) that were based on fibre reinforcement. The analysis was done in term of the increment gained in the load capacity of the wall as a result of the application of the specific retrofit technique. These works were selected for comparison because they presented the same four-point loading scenario and boundary conditions as the one tested in this study. Although the sizes of the walls studied were different, with 1000 x 3000 x 250mm (65), 610 x 1220 x 152mm (66) and 1070 x 2310 x 110mm (67) but the approach of estimating the performance of the proposed retrofit technique is the same. Each study including the present study tested plain specimens as a baseline and estimated the performance of the retrofitted specimens against that. This allows for a fair comparison of the performance of the technique proposed in this study against the existing literature.

Table 4: Performance Comparison of Alternative Retrofit Technique

Reference	Retrofit Technique	Load Capacity (x PW)
This study	Oriented Strand Board (OSB) type 3 on one side (1SRW)	1.4 x PW
This study	Oriented Strand Board (OSB) type 3 on two sides (2SRW)	1.8 x PW
(65)	Externally Bonded Glass Fibre Reinforced Polymer (GFRP)	1.8 x PW
(66)	Fibre Reinforced Cement Mortar (FRCM) Overlay	1.6 x PW
(66)	Near-Surface Mount (NSM) with cementitious additives	1.2 x PW
(67)	Externally Bonded Fibre Reinforced Polymer (FRP)	2.3 x PW

The proposed retrofit technique in comparison with the other existing retrofit techniques performed well in terms of increase of load capacity. The application of glass fibre reinforced polymer (GFRP) by (65) showed load increment of 1.8 times that of the unreinforced wall. Also, the application of fibre reinforced cement mortar (FRCM) and near-surface mount with cementitious additive (NSM) by (66) shows load increment of 1.6 and 1.2 times that of plain wall respectively. (67) also reported a load increment of 2.3 times that of unstrengthened walls when FRP was used to retrofit masonry wall. Even though some of the previous application shows a slightly higher load increment than the proposed technique, in terms of costs, FRP and fibre products are much more expensive than OSB application. Indeed, the cost of applying this proposed OSB technique on a square meter of a masonry wall is estimated (materials and labour) to be £47 for 1SRW and £82 for 2SRW as against £152 estimated for typical fibre-based retrofit applications on 1m² masonry wall.

4. Conclusion

This paper proposes the application of oriented stranded board (OSB) type 3 to retrofit unreinforced masonry walls. It presents an experimental campaign aimed to evaluate the capacity and effectiveness of the proposed timber-based retrofit technique against out-of-plane failure. After an introduction of the overall experimental programme, this paper focuses on the presentation and analysis of six tests performed on 1115 x 1115 x 215mm single leaf, double wythe solid masonry walls. Two of the walls were tested as plain wall (PW), two as single-sided retrofitted masonry wall (1SRW) with the OSB retrofit application on the flexural tension face only, and the last two as double-sided retrofitted masonry wall (2SRW) with the OSB retrofit application on both face of the walls. Out-of-plane bending test in the form of four-point loading test was performed on all the six specimens. The aim was to obtain the response of both the plain and retrofitted masonry walls against out-of-plane loading to evaluate the performance of the proposed technique in terms of out-of-plane resistance (i.e load-carrying and displacement capacities) and the energy absorption (i.e toughness) of both plain and retrofitted walls.

The evaluation of the load-carrying and displacement capacities of both plain and retrofitted walls evidenced significant improvements in the out-of-plane resistance and toughness of masonry wall retrofitted with the OSB panel. The key findings are:

- The application of the OSB timber panel retrofit technique increased the out-of-plane load capacity of the retrofitted wall. The retrofitted masonry wall specimens were able to resist out-of-plane loading which is 1.4times and 1.8times higher than that of plain walls for both 1SRW and 2SRW before the initial crack occurred. Overall, the retrofitted walls were able to resist out-of-plane loading almost 3.0times higher than that of plain walls for both 1SRW and 2SRW and can also resist an out-of-plane displacement that is 6.0times and 3.1times that of PW for 1SRW and 2SRW respectively. A key observation here is that the application of the retrofit on both faces of the wall does not increase the failure load when compared to one side application. However, the load at which the initial crack occurred in 2SRW is 1.4times higher than

the load at which the 1SRW first cracked. Also, the deflection capacity of the double-sided application is higher than the one-sided application.

- The application of the proposed retrofit technique on both sides does affect the toughness of the composite system. The 1SRW absorbed more energy than the 2SRW. This is evident in the ability of the 1SRW to displace more than the 2SRW. Quantitatively, the one-side retrofitted walls were able to absorb energy almost 16times higher than that of plain walls. Meanwhile, the 2SRW can absorb energy, which is 10times higher than that of PW. However, the double-sided application has advantages in term of the limiting toughness and stiffness, showing a better resistant against out-of-plane displacement. The 2SRW also absorbed more energy than 1SRW in the range where the displacement is within the allowable practical limit.
- In term of the observed failure pattern, it emerged that the failure of the PW was sudden with the evolution of crack opening in mortar bed joint almost at the specimens' mid-height. The failure (cracking) abruptly occurred between the interface of the mortar and brick unit, which then cut across the whole specimen thickness. Whereas, the application of the OSB type 3 to retrofit the wall shows that the walls were able to take more loads after the first crack which subsequently led to the formation of other horizontal cracks in the bed joint within the middle thirds of the walls. The failure/collapse of the retrofitted specimens occurred when the applied OSB timber reached their ultimate strain and broken.
- When compared to other retrofit techniques with similar loading scenario and boundary condition, the retrofit with the oriented strand board (OSB) type 3 considerably increased the load and flexural capacity by (1.4 & 1.8times), limiting toughness by (1.6 & 2.4times) and overall toughness by (16 & 10times) that of plain wall subjected to out-of-plane loading for (single & double-sided) application respectively. The application is comparatively cheap (about 30% of the cost of applying fibre-based retrofit techniques).
- The results and observations made in this study were based on specimens that replicate masonry walls without returning walls at the edges. Still, an investigation of the performance of the proposed technique on walls reproducing the in-situ condition of a portion of a typical load-bearing wall with corner walls or slabs is recommended in future. In the meantime, parametric numerical analysis to assess the performance of URM walls retrofitted with different OSB panel thickness, different connection spacing, and different retrofit application position has been carried out by the authors and will be discussed in a future article.

References

1. G. Vasconcelos, P. B. Lourenço, Experimental characterization of stone masonry in shear and compression, *Constr. Build. Mater.* 23 (11) 3337-3(2009) 345, <https://doi.org/10.1016/j.conbuildmat.2009.06.045>.
2. A. Smith, P. Bingel, A. Bown, Sustainability of masonry in construction, In: J. Khatib, ed., *Sustainability of Construction Materials (Second Edition)*, Woodhead Publishing (2016) 245-282, <https://doi.org/10.1016/B978-0-08-100370-1.00011-1>.

3. A. Menon, G. Magenes, Definition of seismic input for out-of-plane response of masonry walls: I. parametric study, *Journal of Earthquake Engineering* 15 (2) (2013) 165-194, <https://doi.org/10.1080/13632460903456981>.
4. C. Wang, J. Forth, N. Nikitas, V. Sarhosis, Retrofitting of masonry walls by using a mortar joint technique: experiments and numerical validation, *Engineering Structures* 117 (2017) 58-70, <http://dx.doi.org/10.1016/j.engstruct.2016.03.001>.
5. S. Nazir, Studies on the failure of unreinforced masonry shear walls. PhD Thesis, Queensland University of Technology (2015).
6. J. Ingham, M. Griffith, The performance of unreinforced masonry buildings in the 2010/2011 Canterbury earthquake swarm August 2011, *Canterbury Earthquakes Royal Commission* (2011), report number: ENG.ACA.0001.
7. N. Gattesco, I. Boem, Out-of-plane behavior of reinforced masonry walls: experimental and numerical study, *Composites Part B: Engineering* 128 (2017) 39-52, <http://dx.doi.org/10.1016/j.compositesb.2017.07.006>.
8. M.J.N. Priestley, Seismic behaviour of unreinforced masonry walls. *Bulletin of the New Zealand National Society for Earthquake* 18 (2) (1985) 191-205.
9. A. A. Costa, A. Arêde, A. Costa, C. Oliveira, Out-of-plane behaviour of existing stone masonry buildings: experimental evaluation. *Bulletin of Earthquake Engineering*, 10 (1) (2011) 93-111, <https://doi.org/10.1007/s10518-011-9332-9>.
10. M. Corradi, A. Osofero, A. Borri, G. Castori, Strengthening of historic masonry structures with composite materials. *Handbook of Research on Seismic Assessment and Rehabilitation of Historic Structures*, (2015) 257-292, DOI: 10.4018/978-1-4666-8286-3.ch008.
11. Y. Pan, D. Xie, S. Yuan, X. Wang, Seismic damages of Nepalese cultural heritage buildings and strengthening measures: case studies on three durbar squares in MS 8.1 Gorkha earthquake, *Harbin Gongye Daxue Xuebao/Journal of Harbin Institute of Technology*, 48 (12) (2016) 172-182.
12. N. Ismail, N. Khattak, Observed failure modes of unreinforced masonry buildings during the 2015 Hindu Kush earthquake, *Earthquake Engineering and Engineering Vibration*, 18 (2) N. (2019) 301-314, <https://doi.org/10.1007/s11803-019-0505-x>.
13. H. Derakhshan, W. Lucas, P. Visintin, M.C. Griffith, Out-of-plane strength of existing two-way spanning solid and cavity unreinforced masonry walls, *Structures*, 13 (2018) 88-101, <https://doi.org/10.1016/j.istruc.2017.11.002>.
14. S. Hamoush, M. McGinley, P. Mlakar, D. Scott, K. Murray, Out-of-plane strengthening of masonry walls with reinforced composite, *Journal of Composites for Construction*, 5 (3) (2001) 139-145.
15. D. D'Ayala, E. Speranza, Definition of collapse mechanisms and seismic vulnerability of historic masonry buildings, *Earthquake Spectra*, 19 (3) (2003) 479-509.
16. L. Decanini, A. De Sortis, A. Goretti, R. Langenbach, F. Mollaioli, A. Rasulo, Performance of masonry buildings during the 2002 Molise, Italy earthquake, *Earthquake Spectra*, 20 (S1) (2004) 191-S220.
17. Y. Lin, D. Lawley, L. Wotherspoon, J. Ingham, Out-of-plane testing of unreinforced masonry walls strengthened using ECC shotcrete, *Structures*, 7 (2016) 33-42, <http://dx.doi.org/10.1016/j.istruc.2016.04.005>.
18. P. B. Lourenço, N. Mendes, A. Costa, A. Campos-Costa, Methods and challenges on the out-of-plane assessment of existing masonry buildings, *International Journal of Architectural Heritage*, 11 (1) (2017) 1-1, <https://doi.org/10.1080/15583058.2017.1237114>.

19. G. Magenes, G. Calvi, In-plane seismic response of brick masonry walls, *Earthquake Engineering & Structural Dynamics*, 26 (11) (1997) 1091-1112, [https://doi.org/10.1002/\(SICI\)1096-9845\(199711\)](https://doi.org/10.1002/(SICI)1096-9845(199711)).
20. S. De Santis, P. Casadei, G. De Canio, G. de Felice, M. Malena, M. Mongelli, I. Roselli, Seismic performance of masonry walls retrofitted with steel reinforced grout, *Earthquake Engineering & Structural Dynamics*, 45 (2) (2015) 229-251, <https://doi.org/10.1002/eqe.2625>.
21. T. Oakley 2017, Car smashes hole through brick wall in Stafford town centre, [Online], Available:<https://www.expressandstar.com/news/localhubs/staffordshire/stafford/2017/07/31/crash-leaves-gaping-hole-in-wall>. [Accessed 29/05/2020].
22. C. Wang, V. Sarhosis, N. Nikitas, Strengthening/retrofitting techniques on unreinforced masonry structure/element subjected to seismic loads: a literature review, *The Open Construction and Building Technology Journal*, 12 (1) (2018), 251-268, doi: [10.2174/1874836801812010251](https://doi.org/10.2174/1874836801812010251).
23. F. Porto, M. Valluzzi, M. Munari, C. Modena, A. Arêde, A. Costa, Strengthening of stone and brick masonry buildings. In: A. Costal, A. Arêde, H. Varum, ed., *Strengthening and retrofitting of existing structures*, 9th ed. Springer: Porto, (2018) 59-75.
24. M. Ferraioli, A. Mandara, Base isolation for seismic retrofitting of a multiple building structure: evaluation of equivalent linearization method, *Mathematical Problems in Engineering*, (2016) 1-17, <http://dx.doi.org/10.1155/2016/8934196>.
25. P. G Asteris, M. P Chronopoulos, C. Z Chrysostomou, H. Varum, V. Plevris, N. Kyriakides, V. Silva, Seismic vulnerability assessment of historical masonry structural systems, *Engineering Structures*, 62-63, (2014) 118-134, <https://doi.org/10.1016/j.engstruct.2014.01.031>.
26. C. Z. Chrysostomou, N. Kyriakides, P. Roussis, P. Asteris, Emerging technologies and materials for the seismic protection of cultural heritage, *Handbook of Research on Seismic Assessment and Rehabilitation of Historic Structures*, (2015) 576-606.
27. S. Brzev, Confined masonry buildings: key components and performance in past earthquake, (2014), [Online], Available At: [Http://www.slideshare.net/eerislides/th1-confined-masonry-svetlana](http://www.slideshare.net/eerislides/th1-confined-masonry-svetlana) [Accessed 15 Jan. 2018].
28. M. Dolce, D. Nigro, F. Ponzio, R. Marnetto, R. The CAM system for the retrofit of masonry structures, In: *Proceedings of 7th International Seminar on Seismic Isolation, Passive Energy Dissipation and Active Control of Vibrations of Structures*, Italy (2001) 485-492.
29. M. ElGawady, P. Lestuzzi, M. Badoux, A review of conventional seismic retrofitting techniques for URM, In: *Proceedings of 13th International Brick and Block Masonry Conference*, Amsterdam (2004) 1-10.
30. P. Jansen, G. Tilly, Wall repair & strengthening (2009), [online], Available at: <http://cintec.com/anchoring-reinforcement/civil-engineering/wall-repair-strengthening-paratec/> [Accessed 12 Dec. 2016].
31. A. Dally, W. Witarnawan, Strengthening of bridges using external post-tensioning (1997), [online] Available at: <https://pdfs.semanticscholar.org/fd7d/9d41fe934af54dc2573106a110c9cf75be33.pdf> [Accessed 7 Apr. 2018].
32. G. Castori, A. Borri, M. Corradi, Behavior of thin masonry arches repaired using composite materials, *Composites Part B: Engineering*, 87 (2016) 311-321, DOI: [10.1016/j.compositesb.2015.09.008](https://doi.org/10.1016/j.compositesb.2015.09.008).

33. R. Fonti, A. Borri, R. Barthel, M. Candela, A. Formisano, Rubble masonry response under cyclic actions: experimental tests and theoretical models, *International Journal of Masonry Research and Innovation (IJMRI)*, 2 (1) (2017), 30-60, DOI: [10.1504/IJMRI.2017.082391](https://doi.org/10.1504/IJMRI.2017.082391).
34. L. Binda, G. Cardani, Seismic vulnerability of historic centres: a methodology to study the vulnerability assessment of masonry building typologies in the seismic area, In: P. Asteris and V. Plevris, ed., *Handbook of Research on Seismic Assessment and Rehabilitation of Historic Structures*. IGI Global, (2015) 213-256.
35. S. Tobriner, *Wooden architecture and earthquakes in Turkey: a reconnaissance report and commentary on the performance of wooden structures in the Turkish earthquakes of 17 August and 12 November 1999*, Report on Earthquake-Safe: Lessons to be Learned, Paris, France (1999).
36. R. Langenbach, From "Opus Craticium" to the "Chicago Frame": earthquake-resistant traditional construction, *International Journal of Architectural Heritage*, 1 (1) (2007) 29-59, <https://doi.org/10.1080/15583050601125998>.
37. M. Pelenur, *Retrofitting the domestic built environment: investigating household perspectives towards energy efficiency technologies and behaviour*, PhD Thesis, University of Cambridge, Queens' College, (2013).
38. I. Giongo, G. Schiro, M. Piazza, On the use of timber-based panels for the seismic retrofit of masonry structures, In: *Proceedings of 3rd International Conference on Protection of Historical Constructions*, Lisbon (2017).
39. M. Giaretton, D. Dizhur, J. Ingham, Shaking table testing of as-built and retrofitted clay brick URM cavity-walls. *Engineering Structures* 125 (2016) 70-79, <https://doi.org/10.1016/j.engstruct.2016.06.032>.
40. D. Dizhur, M. Giaretton, I. Giongo, J. Ingham, Seismic retrofit of masonry walls using timber strong backs. *SESOC Journal* 30 (2) (2017) 1-30.
41. I. Sustersic, B. Dujic, Seismic strengthening of existing concrete and masonry buildings with crosslam timber panels, *Materials and Joints in Timber Structures*, (2014) 713-723, DOI: [10.1007/978-94-007-7811-5_64](https://doi.org/10.1007/978-94-007-7811-5_64).
42. A. Borri, R. Sisti, M. Corradi, Seismic retrofit of stone walls with timber panels and steel wire ropes. *Proceedings of the ICE - Structures and Buildings 0:0*, (2020) 1-14, <https://doi.org/10.1680/jstbu.19.00100>.
43. G. Guerrini, N. Damiani, M. Miglietta, F. Graziotti, Cyclic response of masonry piers retrofitted with timber frames and boards. *Proceedings of the ICE - Structures and Buildings 0:0*, (2020) 54, <https://doi.org/10.1680/jstbu.19.00134>.
44. G. Chen, B. He, Stress-strain constitutive relation of OSB under axial loading: an experimental investigation, *Bioresources*, 12 (3) (2017) 6142-6156, doi:10.15376/biores.12.3.6142-6156.
45. J. Dauda, O. Iuorio, P. Lourenço, Characterization of brick masonry: study towards retrofitting URM walls with timber-panels, In: *Proceedings of 10th International Masonry Conference*, Milan Italy (2018).
46. J. Dauda, P. Lourenço, O. Iuorio, Out-of-plane testing of masonry walls retrofitted with oriented strand board (OSB) timber panels, *Structures and Buildings*, *Journal of Institution of Civil Engineers* (2020), <https://doi.org/10.1680/jstbu.19.00095>.
47. UMINHO, Review on the experimental in-plane and out-of-plane testing. Report on Developing Innovative Systems for Reinforced Masonry Walls, Padova Italy (2006). Available from http://diswall.dic.unipd.it/Results/D5.1_FINAL.pdf.

48. N. Ismail, J. Ingham, In-plane and out-of-plane testing of unreinforced masonry walls strengthened using polymer textile reinforced mortar, *Engineering Structures* 118 (2016) 167-177, <http://dx.doi.org/10.1016/j.engstruct.2016.03.041>.
49. J. Dauda, O. Iuorio, P. Lourenço, Numerical analysis and experimental characterization of brick masonry, *International Journal of Masonry Research, and Innovation (IJMRI)*, 5 (3) (2020) 321-347, DOI: 10.1504/IJMRI.2020.10028163.
50. O. Iuorio, J. Dauda, P. Lourenço, Flexural resistance of masonry wall retrofitted with timber panel under out-of-plane loading, In: *Proceedings of 12th International Conference on Structural Analysis of Historical Constructions, Barcelona Spain (2020)*.
51. A. Reinhorn, A. Madan, Evaluation of tyfo-s fibre wrap system for out-of-plane strengthening of masonry walls, Rep. No 95-AM-0001, Civil Engineering, State University of New York, (1995) [online] Available at: <http://civil.eng.buffalo.edu/~reinhorn> [Accessed 3 Mar. 2017].
52. M. Maheri, M. Najafgholipour, A. Rajabi, The influence of mortar head joints on the in-plane and out-of-plane seismic strength of brick masonry walls, *Iranian Journal of Science and Technology*, 35 (1) (2008) 63-79.
53. H. Derakhshan, J. M. Ingham, M. C. Griffith, Tri-linear force-displacement models representative of out-of-plane unreinforced masonry wall behaviour. In: *Proceedings of 11th Canadian Masonry Symposium, Toronto Canada (2009)*.
54. A. Zeiny, J. Larralde, Seismic evaluation of the performance of retrofitted and repaired brick walls by means of expansive epoxy injection, Department of Civil & Geomatics Engineering & Construction, California State University (2010) [online] Zeiny.net. Available at: <http://zeiny.net/FundedProjects/FoamReport/FoamReport.htm> [Accessed 13 Mar. 2017].
55. T. Bui, A. Limam, D. Bertrand, E. Ferrier, M. Brun, Masonry walls submitted to out-of-plane loading: experimental and numerical study, In: *Proceedings of 8th International Masonry Conference, Dresden (2010)*.
56. A. Costa, A. Arêde, T. Ferreira, A. Gomes, H. Varum, Experimental study of the out-of-plane behaviour of unreinforced sacco stone masonry walls: comparative analysis of two different test setups, In: *Proceedings of 9th International Masonry Conference, (2014)*.
57. H. Maccarini, G. Vasconcelos, H. Rodrigues, J. Ortega, P. Lourenço, Out-of-plane behavior of stone masonry walls: experimental and numerical analysis. *Constr. Build. Mater.* 179 (2018) 430-452, <https://doi.org/10.1016/j.conbuildmat.2018.05.216> 0950-0618.
58. ASTM E72 - 15, Standard test methods of conducting strength tests of panels for building construction, West Conshohocken, PA: ASTM International (2015).
59. ASTM E518 -15, Standard test methods for flexural bond strength of masonry, West Conshohocken, PA: ASTM International (2015).
60. A. Anon, Technical information sheet for oriented strand board (2018) [online] Available: at http://www.osb-info.org/Assets/file/EN/OSB_Technical_Information.pdf [Accessed 02 July 2018].
61. ETAG, ETAG 029-13: Guidelines for European technical approval of metal injection anchor for use in masonry. European Organisation for Technical Approval, Brussel (2013).
62. B. Anon, Brick bonds: heritage directory notes, (2009). [online] Available at: <http://www.theheritagedirectory.co.uk> [Accessed 22 Jan 2017].
63. ASTM C1609 -19, Standard test method for flexural performance of fiber-reinforced concrete (using beam with third-point loading), West Conshohocken, PA: ASTM International (2019).
64. BS EN 1996-1-1:2005: Eurocode 6 -design of masonry structures - part 1-1: general rules for reinforced and unreinforced masonry structures, London: British Standards Institution (1996).

65. I. Boem, Enhancement of the seismic performances of historic masonry buildings through glass fiber-reinforced mortar, PhD Thesis, Università Degli Studi di Trieste (2017).
66. Z. Al-Jaberi, Strengthening of reinforced masonry walls subjected to out-of-plane pseudo-static cyclic load using advanced composite. PhD Thesis, Missouri University of Science and Technology (2018).
67. J. Kashyap, Out-of-plane strengthening of unreinforced masonry walls using FRP, PhD Thesis, The University of Adelaide (2014).